6032 *J. Phys. Chem. A* **2008,** *112,* 6032–6041

Kinetic-Quantum Chemical Model for Catalytic Cycles: The Haber−Bosch Process and the Effect of Reagent Concentration

Sebastian Kozuch* and Sason Shaik*

Institute of Chemistry and The Lise Meitner-Minerva Center for Computational Quantum Chemistry, Givat Ram Campus, Jerusalem 91904, Israel

Received: January 17, 2008; Revised Manuscript Received: March 4, 2008

A combined kinetic-quantum chemical model is developed with the goal of estimating in a straightforward way the *turnover frequency* (TOF) of catalytic cycles, based on the state energies obtained by quantum chemical calculations. We describe how the apparent activation energy of the whole cycle, so-called *energetic span* (δE), is influenced by the energy levels of two species: the *TOF determining transition state* (TDTS) and the *TOF determining intermediate* (TDI). Because *these key species need not be adjoining states*, we conclude that for catalysis *there are no rate-determining steps, only rate determining states*. In addition, we add here the influence of reactants concentrations. And, finally, the model is applied to the Haber−Bosch process of ammonia synthesis, for which we show how to calculate which catalyst will be the most effective under specific reagents conditions.

I. Introduction

Current computational methods, especially those based on density functional theory (DFT), enable the calculations of full catalytic cycles with reasonable accuracy and at moderate costs of computing time. Indeed one can find a good number of such calculations in the current literature.[1] Because the efficiency of a catalytic cycle does not rest on a single step, such calculations can become useful, with a potential of guiding new experiments, only in the advent of methods that connect the theoretical data to the experimentally measurable rates of a given catalyzed reaction under turnover conditions. Derivations of kinetic expressions for catalytic cycles constitute a well-developed area in the community of chemical catalysis. Notable examples include Christiansen's work,[2] Boudart and Dumesic's use of De Donder relations[3,4] or Campbell's degree of rate control.[5,6] The De Donder relations make use of chemical affinities to predict the parameters that delineate the rate of a reaction from its reaction-mechanism scheme, but the method does not take into account the influence of the transition states, as they are not included in the affinities formulation.[7] The degree of rate control adds this information by considering explicitly the impact of each rate constant in the global rate formulation.[5] Although these two formulations are useful, they are not general and must therefore be re-established for each chemical problem.[8] Thus, Christiansen[2] tackled this problem and generated a general solution of the kinetics of catalytic cycles, by considering the kinetic constants of all elementary steps. One of the difficulties with this approach, however, is the growth of the size and complexity of the equations as the square of the number of steps in the cycle. Therefore, a desirable approach is one that can simplify the complexity, and at the same time offers the quantum chemist the means to integrate into this model his/her computational results. In this sense, we have recently used the Christiansen procedure to show that the turnover frequency (TOF), which is the net overall rate of a catalytic cycle, can be expressed in terms of the energetics of its individual steps (see later eq 1) in a simple and general manner that allows a straightforward estimation of the efficiency of catalytic cycles by computational means.

SCHEME 1: Schematic Catalytic Cycle

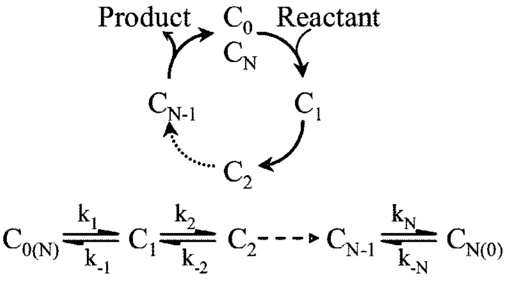

In this work we extend the TOF treatment to include the effect of concentrations of the various species in the cycle. Even though the effect of concentrations on rates is secondary to the energies of the states (linear dependence vs exponential), the consequences of modulating the concentrations of reactants and products are nevertheless significant. To demonstrate the impact of concentrations on the TOFs of catalytic cycles, we apply the newly derived expressions to elucidate the factors that control the effectiveness of the catalyst in the Haber−Bosch process of ammonia synthesis or its degradation.[9,10]

II. Theory of Catalytic Cycles

As an introduction to the theory, we shall repeat some elements of the derivation we published in the past for normalized concentrations (in parts A−C).[11] Subsequently, in part D we shall introduce the effect of concentration and in section III we shall discuss catalytic effectiveness as a function of the concentrations by revisiting the Haber−Bosch process. To avoid an unnecessary blizzard of equations, we relegated the full derivations to Appendix 1, and in what follows we present the key features of the model.

A. TOF Calculations from Energy Levels. A simple catalytic cycle, as the one shown in Scheme 1 and in Figure 1 in a steady state regime, is typified by a global rate, the so-

---

* Corresponding authors. E-mail: kozuchs@yfaat.ch.huji.ac.il.

10.1021/jp8004772 CCC: $40.75

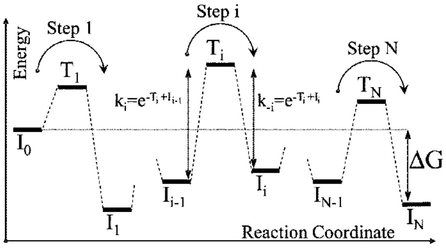

Figure 1. *N* steps in a catalytic cycle. T_i corresponds to the transition state energy of step *i*, and I_i is the following intermediate energy. ΔG is the reaction energy, independent of the catalyst.

called turnover frequency (TOF), which is the net rate of product formation under conditions of standard 1 M concentrations of the catalyst, as expressed in ref 11 and shown in eq 1

$$\mathrm{TOF} = \frac{\Delta}{M} = \frac{\mathrm{e}^{-\Delta G} - 1}{\sum_{i,j=1}^{N} \mathrm{e}^{T_i - I_j - \delta G'_{i,j}}} \tag{1}$$

$$\delta G'_{i,j} = \begin{cases} \Delta G & \text{if } i > j \\ 0 & \text{if } i \le j \end{cases}$$

The energies (T_i and I_j) above and in all subsequent equations are dimensionless quantities expressed in k_bT units (e.g., $I_i = G(I_i)/k_bT$, where $G(I_i)$ is the free energy of the *i* intermediate), and the units of TOF are in s^{-1}, the usual rate constant units. Thus, by analogy to Ohm's law, the TOF is the "net molecular flux" that generates products and is given by the ratio of the driving force Δ, and the "resistance" *M* to this "flux". The "driving force" of the reaction flux, Δ, is independent of the nature of the catalyst and is a function of ΔG, the free energy of the reaction, and as such Δ is independent of the reaction mechanism; the -1 term in the numerator provides thermodynamic balance: when $\Delta G = 0$, the Δ and TOF quantities must be zero for standard concentrations (see Appendix 1). *M*, the "resistance" to the "molecular current", is catalyst dependent and a function of the state energies, of the intermediates (I_j) and transition states (T_i), which appear on the energy landscape of the cycle. The better the catalyst, the lower the resistance to the catalytic flux and the larger is the TOF. Details of the derivation of eq 1 are given in Appendix 1. It is important to clarify the following points: (a) There are two different representations, the rate-constant representation (eqs a7 and a8 in the Appendix), and the energy-representation given above in eq 1. Both representations correspond to a steady state regime, and the energy representation is also treated by transition state theory where all the pre-exponential factors in the rate constants are identical (k_bT/h). In the specific case, where some of the pre-exponential factors differ from k_bT/h, this feature can be easily incorporated into the model. (b) The energy differences in the denominator *M* in eq 1, involves all the possible energy differences between all the transition states and all the intermediates appearing in the cycle. This is a consequence of the products of the rate constants in the rate-constant representation (see eq a8).

B. Degree of TOF Control ($X_{\mathrm{TOF},i}$). The *degree of TOF control* specifies the sensitivity of the TOF to a change in the energy of a specific state of the cycle[4,5,11] and is defined as follows:

$$X_{\mathrm{TOF},i} = \left| \frac{1}{\mathrm{TOF}} \frac{\partial \mathrm{TOF}}{\partial E_i} \right| \tag{2}$$

where E_i is a dimensionless free energy of a transition state (T_i) or an intermediate (I_i). In this expression the $X_{\mathrm{TOF},i}$ varies between the limits of one (full dependence of the TOF on state *i*) and zero (totally independent TOF with a change in that state). On the basis of eq 1, the resulting expression becomes

$$X_{\mathrm{TOF},T_i} = \frac{\sum_j \mathrm{e}^{T_i - I_j - \delta G'_{ij}}}{\sum_{ij} \mathrm{e}^{T_i - I_j - \delta G'_{ij}}} \qquad X_{\mathrm{TOF},I_j} = \frac{\sum_i \mathrm{e}^{T_i - I_j - \delta G'_{ij}}}{\sum_{ij} \mathrm{e}^{T_i - I_j - \delta G'_{ij}}} \tag{3a}$$

$$\sum_i X_{\mathrm{TOF},T_i} = 1 \qquad \sum_j X_{\mathrm{TOF},I_j} = 1 \tag{3b}$$

A useful relationship is that the sum of all the $X_{\mathrm{TOF},i}$ for the transition states or for the intermediates is always one, as shown in eq 3b. This means that changing one state will change the influence on the TOF of all the other states in a complementary manner.[4,5,11]

In many catalytic cycles, albeit not always, we can find two states, one intermediate and one transition state, which possess the largest TOF control parameters and are, hence, the key species that determine the TOF of the catalytic cycle. The intermediate with higher $X_{\mathrm{TOF},I}$ will be referred to in the present paper as the TOF-Determining Intermediate, TDI,[12] whereas the transition state with $X_{\mathrm{TOF},T}$ closer to one will be called the TOF-Determining Transition State, TDTS.[13] As the TDI and the TDTS are not necessarily adjoining states, it is important to recognize that in the light of this model in catalytic cycles *there are no rate-determining steps*, only *rate determining states*. It is very important to stress the meaning of this statement: saying that the occurrence that two nonadjoined states in a given cycle will determine the TOF is equivalent to a statement that the TOF in the rate-constant representation is determined by a product of rate constants of elementary steps (see eq a8). Therefore, the energy-representation of TOF makes things much clearer by identifying the states that determine the kinetics of the cycle.[5]

C. Apparent Activation Energy of the Cycle (the Energetic Span Approximation). For an exothermic reaction the exponential of the reaction energy ($\mathrm{e}^{-\Delta G}$) is much greater than one, so the unity term in eq 1 can be neglected. Considering the denominator of eq 1, usually only one term in the summation will be dominant. This leads to a very simple equation for the TOF of a cycle in eq 4, using the rate constant representation of TOF:

$$\mathrm{TOF} \approx \mathrm{e}^{-\delta E} \tag{4}$$

Here, δE, so-called the *energetic span of the cycle,*[11,14] is the apparent activation energy of the cycle and is given by eqs 5a and 5b (see Figure 2):

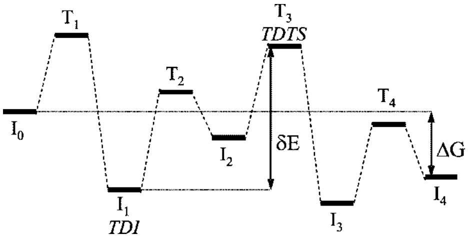

Figure 2. Schematic cycle exemplifying TDTS (T_3) and TDI (I_1). Note that these states are not adjoined, nor are they the highest and lowest points in the graph, but the ones that maximize the effective activation energy of the cycle, δE (eq 5a). T_1 and I_3 are the extreme states in the cycle but are not the TOF determining states because the T_1 precedes I_3 (eq 5b), and the corresponding energy difference relation is lowered by ΔG; thus mathematically, $\delta E = T_3 - I_1 > T_1 - I_3 + \Delta G$.

$$\delta E = \begin{cases} T_i - I_j & \text{if } i > j \quad \text{(a)} \\ T_i - I_j + \Delta G & \text{if } i \le j \quad \text{(b)} \end{cases} \tag{5}$$

T_i and I_j in the equation are the energies of the states that maximize the energetic span (the TDI and TDTS). Note that the apparent activation energy has a different expression depending on whether the TDTS (T_i) follows the TDI (I_j), eq 5a, or precedes it, eq 5b. In fact, because of the ΔG term in eq 5b, these states are not necessarily the highest and lowest energy levels of the cycle. This arises due to the "cyclic" Ouroboros-like nature of the catalytic process. The schematic representation in Figure 2 shows that by considering all the possible pairs of transition state and intermediates, one finds that I_1−T_3 maximizes the span, because other pairs where T_i precedes I_j involve the ΔG term that reduces the span. Thus, finding the TDI and TDTS requires considering all the possible pairs in light on eqs 5a and 5b. Appendix 2 shows a visual aid that achieves this identification (an Excel file that calculates the TOF from the energy states is provided as Supporting Information and is available from the authors upon request).

Once we identify the TDTS and the TDI and we know the ΔG of the cycle, we have (in this approximation) all the needed kinetic information for the global rate of the cycle. The rate of the full reaction, the influence of a small change in the catalyst structure or even the kinetic isotope effect can be derived from the energetic span model in a much simpler way than having to calculate the rate equation from rate constants. As we already wrote above, the energy viewpoint has in this way several advantages compared to the rate constant perspective.

It is clear then that to improve the efficiency of a catalytic cycle we have to search for a catalyst that lowers the TDTS without changing the TDI, or vice versa, a catalyst that raises the TDI while maintaining the energy level of the TDTS. In this light, we emphasize that a catalyst that generates lower transition states will not necessarily be a better one, as such a catalyst will usually lower also the intermediates, and thereby unaffecting the TOF.[11,15] Cycle kinetics is not a function of a single elementary step and therefore requires consideration of the entire reaction profile. Quantum chemistry is an ideal tool for charting the entire energy landscape.

An illustrative example of how to apply the model expressions, is the classic catalytic degradation of ozone by chlorine atoms (Scheme 2),[16] for which there is a DFT calculation of the entire cycle[17] (see also Figure 3).

SCHEME 2: Cycle for Ozone Degradation by Cl•

$$\begin{array}{rcll} {}^2\mathrm{Cl} + {}^1\mathrm{O}_3 & \rightleftharpoons & {}^2\mathrm{ClO}_3 & (1) \\ {}^2\mathrm{ClO}_3 & \rightleftharpoons & {}^2\mathrm{ClO} + {}^3\mathrm{O}_2 & (2) \\ {}^2\mathrm{ClO} + {}^3\mathrm{O} & \rightleftharpoons & {}^4\mathrm{ClO}_2 & (3) \\ {}^4\mathrm{ClO}_2 & \rightleftharpoons & {}^2\mathrm{Cl} + {}^3\mathrm{O}_2 & (4) \end{array}$$

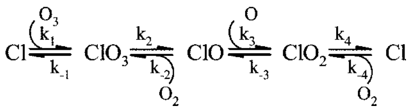

In this model there are four intermediates and four transition states, which make 16 terms in the summation M in the denominator of eq 1 (see Appendix 1, eq a8). Steps 1 and 2 are diffusion controlled, and T_1, T_3, I_0 and I_2 have very low degrees of TOF control. This leaves us with a TOF calculation for this cycle of

$$\mathrm{TOF}_{\mathrm{Cl/O_3}} = \frac{e^{-\Delta G} - 1}{e^{T_2 - I_1 - \Delta G} + e^{T_4 - I_1 - \Delta G} + e^{T_2 - I_3} + e^{T_4 - I_3 - \Delta G}}$$
$$T_2 = -40.90/RT \qquad T_4 = -47.73/RT \tag{6}$$
$$I_1 = -43.31/RT \qquad I_3 = -48.70/RT$$
$$\Delta G = -102.72/RT$$

A close inspection of eq 6 shows that the first term in the denominator is also the largest, and thus T_2 (oxygen abstraction) and I_1 (${}^2\mathrm{ClO}_3$) are the TDTS and TDI in the ozone degradation. The energetic span will be then T_2−I_1 = 2.41 kcal/mol, i.e., an extremely fast reaction with a large TOF. In this example, the two states are adjoined and belong to a single elementary step, but in the general case they may be nonadjoined and separated by a few states (see, e.g., Figure 2).

D. Influence of Reactants and Products Concentrations. As we wrote already, a heuristically useful way of conceptualizing a catalytic cycle is as a net molecular flux that is constantly fed by reactants and its outputs are the products. Generally, a catalytic cycle may have a few different reactants that are inputted in different steps leading to various products. An example is the cycle shown above in Figure 3. Another example, is the cycle of an enzyme like cytochrome P450,[18,19] which leads to substrate oxidation, by using molecular oxygen, reducing equivalents and protons, which are inputted in different stages of the cycle and lead to products and byproducts in different sections of the cycle. Scheme 3 shows such a general cycle that considers the influence of reactants (R_h) and products (P_h), which participate in the net reaction, $R_1 + R_2 + ... + R_N \rightarrow P_1 + P_2 + ... + P_N$.

SCHEME 3: Cycle with Input of Reactants (R_h) and Output of Products (P_h) at Different Stages

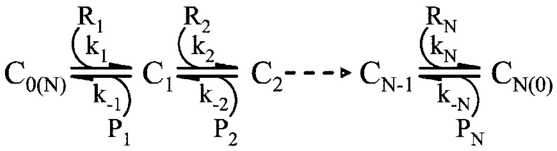

Taking into account the variable concentrations of R_h and P_h leads to the following expression in eq 7:

$$\mathrm{TOF} = \frac{e^{-\Delta G}\prod_h [R_h] - \prod_h [P_h]}{\sum_{i,j} e^{T_i - I_j - \delta G'_{i,j}} \prod_h \delta R'_{h,i,j} \cdot \delta P_{h,i,j}} \tag{7}$$

The equation differs from eq 1 above by having the concentrations of reactants R_h and products P_h as multipliers of the energy dependent terms in eq 1 (details of the derivation are given in Appendix 1). The term $\delta R'_{h,i,j}$ in the denominator of eq 7 is either $[R_h]$ or 1, and so is the case for the term $\delta P_{h,i,j}$. Thus, as a rule, a specific reactant concentration term $[R_h]$ will enter the

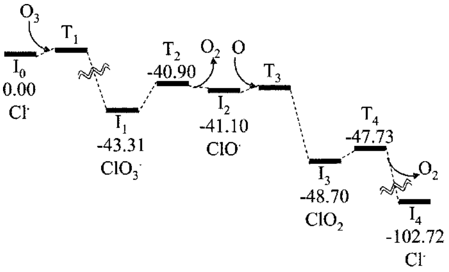

Figure 3. Computed[17] reaction profile of ozone degradation. Free energies are in kcal/mol.

equation in the denominator term when the reactant R_h is consumed in a chemical step *other than* the one spanned from the intermediate I_j to the transition state T_i (ordered in a clockwise manner). In contrast, the product concentration $[P_h]$ enters the denominator whenever it is generated in the step that proceeds from I_j through T_i.

To exemplify the use of eq 7, let us turn back to the ozone example (eq 6, Scheme 2, and Figure 3) and consider the TOF expression including concentrations. The numerator of the TOF (Δ) has in the first term concentrations for all the reactants, and in the second term for all the products, giving for this example:

$$\Delta = e^{-\Delta G}[O_3][O] - [O_2]^2 \tag{8}$$

The denominator (M) in eq 7 involves four terms corresponding to the combinations of T_2, T_4 and I_1, I_3:

$$M = e^{T_2-I_1-\Delta G}[O_3][O] + e^{T_4-I_1-\Delta G}[O_2][O_3] + e^{T_2-I_3}[O_2][O] + e^{T_4-I_3-\Delta G}[O_3][O] \tag{9}$$

The first term refers to the section of the cycle involving I_1 and T_2. On the basis of the above rule, this term will contain the reactant concentrations that are not consumed in this section of the reaction (O_3 and O; see Figure 3). Because in the section I_1 to T_2 no product is produced, the first term in eq 9 does not have products concentration. The second term in M refers to the reaction that proceeds from I_1 to T_4, where O_2 is produced, and this term enters the expression, while the O atom is consumed in this section and is hence not appearing in the equation. Finally, the reactant O_3, which does not participate in this section, is included in the expression. Following the same reasoning one can deduce the concentrations included in the remaining terms of the equation.

Next we exemplify the effect of concentration using the energetic span approximation in 4, which involves only two TOF-controlling species called TDI and TDTS. In this case the approximate TOF takes the following expression (see Appendix 1):

$$\mathrm{TOF} \approx e^{-\delta E} \prod_h \frac{\delta R_{h,x,y}}{\delta P_{h,x,y}} \tag{10}$$

where now the reactants and products that appear in this approximate equation are the ones that are respectively consumed and produced between the TDI (labeled here as intermediate y) and the TDTS (the TS indexed by x). This means that a reactant that is consumed between the TDI and the TDTS will enhance the reaction rate at high concentration, whereas the products generated in this section of the cycle will lower the TOF in high concentration. In this approximation all other reactant and product species do not affect the overall kinetics.

Taking again our example the ozone cycle and recalling that the first term in the denominator is the most influential, we get

$$\mathrm{TOF}_{\mathrm{Cl/O_3}} = \{e^{-\Delta G}[O_3][O] - [O_2]^2\}/\{e^{T_2-I_1-\Delta G}[O_3][O] + e^{T_4-I_1-\Delta G}[O_2][O_3] + e^{T_2-I_3}[O_2][O] + e^{T_4-I_3-\Delta G}[O_3][O]\}$$
$$\approx \frac{e^{-\Delta G}[O_3][O]}{e^{T_2-I_1-\Delta G}[O_3][O]} = e^{-T_2+I_1} \tag{11}$$

Note that in this approximation, ozone degradation is seen to be largely independent of concentration changes. However, it must be stressed that this example was chosen to illustrate how to apply the approximation, but the application to the actual process may be unrealistic for several reasons: As the radical concentrations are extremely low, we cannot neglect any step for the purpose of using the energetic span approximation. In addition, we are considering steady state kinetics, within transition state theory and assuming there is fast relaxation of the intermediates. These conditions may not apply for this gas phase process. Let us then turn to another application, which might be somewhat more realistic.

III. Why Do the Forward and Reverse Reactions Need Different Catalysts? The Example of NH_3 Synthesis

The celebrated Haber–Bosch process for ammonia's production is still under continuous research after almost a century of its formulation. An intriguing recent result highlighted the fact that the effectiveness of NH_3 formation by means of heterogeneous catalyst varies at different concentrations of reactants and products.[9,10] The extreme case occurs when comparing the synthesis (forward reaction) and degradation (reverse reaction) of ammonia. For this specific case the kinetic results[9,10] show that the reason of this variable catalytic behavior lies in the adsorption energy of the reactants on a given metal surface, assuming identical mechanisms for all metals. Herein we present a physical explanation of this effect based on the energetic span model in conjunction with the Brønsted–Evans–Polanyi (BEP) relationship.[20] In so doing we introduce a new element in the kinetic theory of catalytic cycles that can account and predict which catalyst will be the most effective for the specific concentrations of the reaction. Part A starts by searching for the best catalyst in ammonia synthesis and degradation through consideration of the chemisorption energy. In part B a generic catalytic cycle is revisited to find the optimal catalyst for specific medium conditions.

A. Finding the Best Catalyst for the Synthesis and Degradation of Ammonia. In a grossly simplified representation of the Haber–Bosch process we can express the synthesis of ammonia as follows in Scheme 4, where the asterisk means an active site on the surface of the catalyst, and the process in the scheme considers eight such sites, one for each atom. As considered before, the factor that distinguishes, between efficient catalysts for the "forward" vis-à-vis the "backward" processes, is the exothermicity of the chemisorption step. In heterogeneous catalysis this is the "adsorption energy" (A_E) of the reactant to the surface. In Figure 4 we show two energy profiles; one describing exothermic ($A_E < 0$) and the other endothermic ($A_E > 0$) adsorptions.

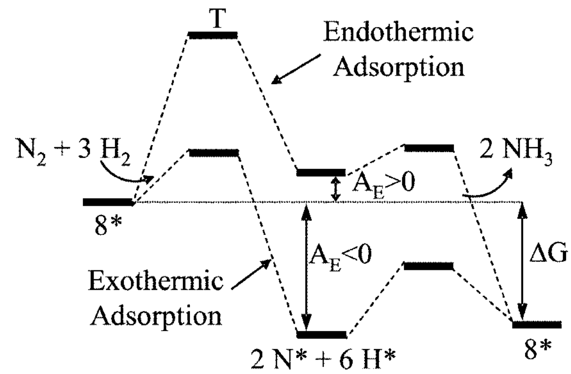

Figure 4. Two model catalysts for the same mechanism reaction (the lower with exothermic adsorption, the higher with an endothermic one).

SCHEME 4: Simplified Haber–Bosch Process

$$N_2 + 3\,H_2 + 8^* \rightleftharpoons 2\,N^* + 6\,H^* \rightleftharpoons 2\,NH_3 + 8^*$$

As the TS for the chemisorption is the TDTS for the process, then using the energetic span model (eq 7), the TOF becomes

$$\mathrm{TOF} = \frac{e^{-\Delta G} p_{H_2}^{\ 3} p_{N_2} - p_{NH_3}^{\ 2}}{e^{T-A_E} p_{NH_3}^{\ 2} + e^{T-\Delta G}} \qquad (12)$$

Here the first term of the denominator is relevant for exothermic adsorption reactions, and the second term becomes important for endothermic adsorption ones.

When the total pressure is fixed, the partial pressure of ammonia (p_{NH_3}) will dictate the tendency to produce ammonia (low p_{NH_3}, positive TOF) or decompose it (high p_{NH_3}, negative TOF). Let us see the effect of modifying the concentration of ammonia on the performance of a highly exothermic adsorption energy catalyst ($A_E \ll \Delta G$) such as Fe or Mo.[10,21] In this case we can neglect the second term in the denominator of eq 12. The resulting TOF will be

$$\mathrm{TOF}_{\mathrm{exo}} = \frac{e^{-\Delta G} p_{H_2}^{\ 3} p_{N_2} - p_{NH_3}^{\ 2}}{e^{T-A_E} p_{NH_3}^{\ 2}} = \left(\frac{K}{Q} - 1\right) e^{-T+A_E}$$

$$K = e^{-\Delta G} \qquad Q = \frac{p_{H_2}^{\ 3} p_{N_2}}{p_{NH_3}^{\ 2}} \qquad (13)$$

Note that when the pressure quotient Q is equal to K (at thermodynamic equilibrium), the $\mathrm{TOF}_{\mathrm{exo}}$ is equal to zero, as expected.

In a situation of a catalyst with high endothermic adsorption energy ($A_E \gg \Delta G$) like Ni or Cu,[10,21] the neglected term is the first one in the denominator of eq 12, so the TOF becomes

$$\mathrm{TOF}_{\mathrm{endo}} = \frac{e^{-\Delta G} p_{H_2}^{\ 3} p_{N_2} - p_{NH_3}^{\ 2}}{e^{T-\Delta G}} = \left(\frac{1}{Q} - \frac{1}{K}\right) p_{NH_3}^{\ 2}\, e^{-T} \qquad (14)$$

where again at thermodynamic equilibrium $\mathrm{TOF}_{\mathrm{endo}} = 0$.

Consider the system with total pressure maintained at 1 bar and the temperature at 773 K, with an N_2:H_2 ratio of 1:3. Under these conditions the thermodynamic equilibrium will be at 0.13% of NH_3.[10] If we plot the calculated TOF for these external conditions (Figure 5, eqs 13 and 14), we reach a clear-cut conclusion: In the synthesis reaction, with low NH_3 pressure (left side in Figure 5), a catalyst with exothermic adsorption is by far more efficient than an endothermic one, which can hardly be called a catalyst at low p_{NH_3}. The opposite applies to the decomposition reaction (right side of Figure 5), and a catalyst that leads to an endothermic adsorption is the only choice at high concentration. Therefore, we can see that for the extreme concentration conditions, extreme catalysts are desirable. More important, we must bear in mind that no catalyst can be universal for a given reaction. Not only the mechanism defines the desirable catalyst, but also the medium settings.

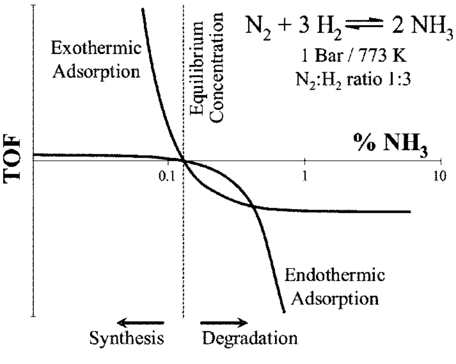

Figure 5. TOF vs percentage of NH_3, for exothermic (eq 13) and endothermic (eq 14) adsorption for the Scheme 4 reaction.

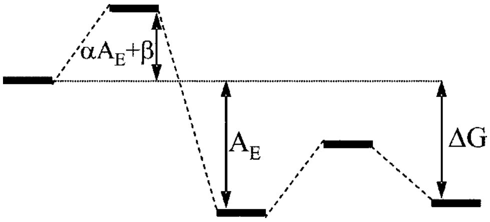

Figure 6. TDTS with energy variation that obeys a BEP relation to the adsorption energy change.

Nevertheless, for a specific concentration the most efficient catalyst must have a specific A_E. Thus, if the energy of the TDTS is related to the adsorption energy by the BEP principle (a linear relationship; see Figure 6), then we may write that

$$T = \alpha \cdot A_E + \beta \qquad 0 < \alpha < 1 \qquad (15)$$

where α and β are characteristic constants of the mechanism.

To obtain the maximum possible TOF, namely locate the most efficient catalyst, we must minimize the "resistance" of the reaction, M (eqs 1 and 12) with respect to A_E, where A_E is the characteristic property of the catalyst:

$$\mathrm{TOF} = \frac{\Delta}{M} = \frac{e^{-\Delta G} p_{H_2}^{\ 3} p_{N_2} - p_{NH_3}^{\ 2}}{e^{T-A_E} p_{NH_3}^{\ 2} + e^{T-\Delta G}} = \frac{e^{-\Delta G} p_{H_2}^{\ 3} p_{N_2} - p_{NH_3}^{\ 2}}{e^{(\alpha-1)A_E+\beta} p_{NH_3}^{\ 2} + e^{\alpha A_E+\beta-\Delta G}} \qquad (16)$$

$$\frac{\partial M}{\partial A_E} = 0 = (\alpha - 1) e^{(\alpha-1)A_E+\beta} p_{NH_3}^{\ 2} + \alpha \cdot e^{\alpha \cdot A_E+\beta-\Delta G} \qquad (17)$$

This means that the best catalyst for this reaction is the one having adsorption energy given by

$$A_{E,\max} = \ln \frac{1-\alpha}{\alpha} - \Delta G + 2 \ln p_{NH_3} \qquad (18)$$

Here $A_{E,\max}$ depends on the logarithm of the product concentration (pressure), but independent of the reactant concentration (pressure). This effect originates from the quasi-equilibrium between the intermediate and the final state. The reaction product can occupy most of the sites of the catalyst when having an exothermic adsorption, thereby inhibiting the reaction. In contrast, in the case of low product concentration, the more critical factor is the activation energy of the first step.

Figure 7 shows the calculated curves of TOF vs adsorption energy, at different ammonia percentage constructed from eq 16. The obtained curves are referred to as Sabatier's volcanoes.[9,21] These volcanoes show the effect of the metal surface to the TOF. At first, when the chemisorption energy grows (by changing the metal), so does the TOF, up to a maximum value that defines the most effective catalyst. This is so because at very low A_E the reactants are tightly stuck to the surface and limit the number of active sites. But beyond the apex of the volcano, a higher A_E value is detrimental, in view of the fact that the TS energies also grow, as described by the BEP principle (eq 15). An explanation of TOF volcano's shape in the energetic span model can be obtained in ref 11. As expected, this "most effective catalyst" (the one whose adsorption energy corresponds to the maximum in the volcano) changes with the

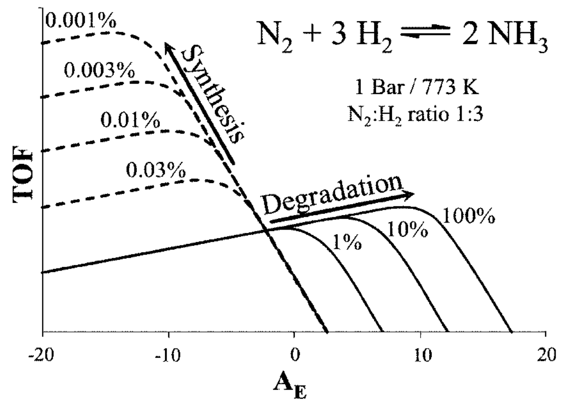

Figure 7. Volcano-shaped TOF curves as function of adsorption energies, from eq 16; BEP parameters: $\alpha = 0.9$, $\beta = 46$ kcal/mol.[22] A_E is the adsorption energy of the reactants to different metal surfaces. Solid lines represent ammonia degradation, and dashed lines describe ammonia synthesis, at specified ammonia percentage. The maximum of each volcano corresponds to eq 18.

concentrations as shown in eq 18. Here, the A_E for the maximum TOF grows as twice the logarithm of pressure of ammonia.

It must be noted that these curves correspond to the extremely simplified mechanism of Scheme 4, which duly lead to trends that are qualitative rather than quantitative. Accurate calculations of Boisen et al.[10] shows a linear relation to $\ln(p_{NH_3})$ with a slope of 2.8.

B. Finding the Best Generic Catalyst. Let us consider a generic two-steps catalytic cycle like in Scheme 5, where we may have a heterogeneous or a homogeneous reaction.

SCHEME 5: Generic Two-Step Cycle

$$R + C \rightleftharpoons RC \rightleftharpoons n\,P + C$$

Following the same line of arguments of the previous section, we can seek the best catalyst for each reaction that follows this generic mechanism. Here, the energy level of the intermediate by reference to the starting point can be the substrate-binding state for an enzyme, the ligation of the reactants in organometallic catalysis or like in the ammonia process discussed previously, the adsorption energy. So we will label this energy difference A_E like before (see Figure 6).

If the TDTS occurs in the first step like in the Haber–Bosch process as in Figure 4, and by the same treatment (see eqs 15–18), the maximum TOF will be achieved under the following condition:

$$A_{E,\max} = \ln\frac{1-\alpha}{\alpha} - \Delta G + n\ln[P] \qquad T_1 \rightarrow \text{TDTS} \qquad (19)$$

So again, the best catalyst for a reaction that follows a simplified two-steps mechanism, as the one in Figure 6, where the first transition state is the most influential one, will be the one with an A_E corresponding to eq 19. This means that if we want the best catalyst all along the reaction, we may have to change it as a function of the logarithm of the product concentration. In a batch reactor this may require to substitute the catalyst by one leading to a higher intermediate energy, as the reaction time and the product concentration grows. In a plug flow reactor this may mean putting different catalysts along the flow path, each one with higher A_E than the previous one.

In the case of a reaction where the second transition state is the TDTS (as in Figure 8), the quasi-equilibrium is established between the reactant and the adsorbed/bound intermediate. This type of reaction corresponds for example to an organometallic catalyst with a reductive elimination as determining TS, desorption in heterogeneous chemistry, or an enzymatic process with small k_2 in the Michaelis–Menten scheme (see Appendix 3). By the same deduction as before (eqs 15–19), we get the following expression for the adsorption energy:

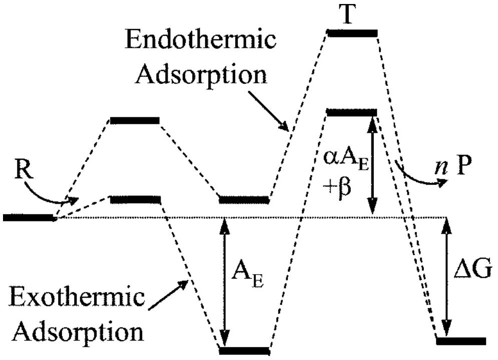

Figure 8. Two-step reaction as in Scheme 5, with the second transition state as the TDTS.

$$A_{E,\max} = \ln\frac{1-\alpha}{\alpha} + \ln[R] \qquad T_2 \rightarrow \text{TDTS} \qquad (20)$$

In this situation with the second TS being TOF determining, as the reactant concentration declines along the reaction, we should seek new catalysts with lower adsorption energy for maximum effectiveness (eq 20). This corresponds to an opposite trend compared with the case where the first TS is the TDTS (eq 19). Therefore, there is no universal catalyst for a given mechanism. The optimum catalyst depends on state energies as well as on concentrations of reactants, intermediates and products.

IV. Conclusion

We present here a simple equation based on the energy-representation that permits the direct calculation of the turnover frequency (TOF) of catalytic cycles using the states in the cycle (eq 1). This enables one to calculate the TOF from the theoretically computed energy landscape, and to include in addition the impact of reactants and product concentrations (eq 7). This equation is fully equivalent to the rate-constant representation of the TOF (eq a8), where the TOF is expressed in terms of kinetic rate constants. The energy representation is simpler and more revealing, and it is useful for quantum chemists. From this TOF expression and its simplified form (eqs 4, 5 and 10), it is possible to derive the key states that control the kinetics of the cycle. Thus, the apparent activation energy of the cycle (see eqs 4 and 5), depends on two states: the most influential transition state (the TDTS) to the dominant intermediate (the TDI); their energy difference is the apparent activation energy of the cycle (see eqs 4 and 5), also-called the energetic span of the cycle. A central inference of the energetic span model is the following: *in catalysis there are no rate determining steps, but rate determining states.* This means that the TDTS and the TDI need not be adjoined via single elementary step of the cycle; they can be separated by as many states as needed as long as they maximize the energetic span (eq 5). Furthermore, these states need not be the highest TS and lowest intermediate. Thus, the use of the term "rate-determining step" in a catalytic cycle is not correct in the general case. The conclusion is clearer from the energy-representation of the TOF for catalytic cycles, whereas in the rate-constant representation (eq a8) the TOF will be determined by products and/or quotients of rate constants of the elementary steps. Therefore, the analysis of a catalytic cycle must rest on the full energy graph of the cycle. An ideal tool for this purpose is quantum chemistry.[1] Subsequent use of eq 5, will lead to the expression of the TOF and to the identity of the two critical states that have to be influenced to affect the overall kinetics.

When the reactant and product concentrations are added to the equations (based on the energetic span approximation), we find that the only species that affect the TOF are the ones that are consumed or produced within the section of the cycle that starts in the TDI and ends in the TDTS (eq 10). An example of the effect of the concentrations is provided by the general problem of defining the most efficient catalyst for a given process. With the addition of the Brønsted−Evans−Polanyi relationship (eq 15) to the TOF equation, it was shown that the best catalyst is not universal but dependent on the medium concentrations (eqs 19 and 20). The different effectiveness of heterogeneous catalysts on the ammonia synthesis (Haber−Bosch process) and degradation was explained using this model.[24]

Appendix 1: Expression Derivations

TOF for Simple Catalytic Cycles. Although rate constants (k's) are the *lingua franca* of experimentalists, in QM calculations all states are described in terms of their relative energies, in a reaction profile that is located during the computational procedure. A connection between energies and rate constants is given by the Eyring expression:

$$\begin{aligned} k'_i &= \frac{k_B T}{h} e^{-\Delta G^{\ddagger}_i/k_b T} = \frac{k_B T}{h} e^{G(I_{i-1}) - G(T_i)/k_b T} \\ k'_{-i} &= \frac{k_B T}{h} e^{-\Delta G^{\ddagger}_{-i}/k_b T} = \frac{k_B T}{h} e^{G(I_i) - G(T_i)/k_b T} \end{aligned} \tag{a1}$$

For convenience, we can use the energies in k_bT units ($I_i = G(I_i)/k_bT$ for the intermediates, $T_i = G(T_i)/k_bT$ for the transition states, where $G(I_i)$ and $G(T_i)$ are Gibb's free energies, according to the transition state theory) and define the k's in k_BT/h units ($k_i = k'_i h/k_BT$) to obtain the following expressions for the rate constants:

$$\begin{aligned} k_i &= e^{I_{i-1} - T_i} \\ k_{-i} &= e^{I_i - T_i} \end{aligned} \tag{a2}$$

Throughout this work we used these dimensionless energy units (unless specified differently). Also, when not specified, concentrations and pressures are considered respective to the standard 1 molar and 1 bar.

In a simple catalytic cycle (Scheme 1) a steady state can be expressed by considering the invariance in the catalytic intermediates with time:

$$\frac{d[C_i]}{dt} = k_i[C_{i-1}] - k_{-i}[C_i] = 0 \tag{a3}$$

Expressing these relations for all the intermediates generates a nonsingular N equations system. Adding the sum of all the catalyst species concentrations as equal to one (i.e., normalized) for a TOF calculation, the matrix representation of a simple cycle with four intermediates is

$$\begin{pmatrix} k_1 & -(k_{-1} + k_2) & k_{-2} & 0 \\ 0 & k_2 & -(k_{-2} + k_3) & k_{-3} \\ k_{-4} & 0 & k_3 & -(k_{-3} + k_4) \\ 1 & 1 & 1 & 1 \end{pmatrix} \begin{pmatrix} [C_0] \\ [C_1] \\ [C_2] \\ [C_3] \end{pmatrix} = \begin{pmatrix} 0 \\ 0 \\ 0 \\ 1 \end{pmatrix} \tag{a4}$$

or in shorthand matrix notation $\hat{A} \cdot \vec{C} = \vec{I}$. By Cramer's rule the resolution is straightforward:

$$[C_i] = \frac{\det \hat{A}_i}{\det \hat{A}} \tag{a5}$$

where $\hat{A}_i$ is constructed changing the column i of matrix $\hat{A}$ by vector $\vec{I}$. The TOF calculation is then

$$\mathrm{TOF} = k_i[C_{i-1}] - k_{-i}[C_i] = \frac{k_i \det \hat{A}_{i-1} - k_{-i} \det \hat{A}_i}{\det \hat{A}} = \frac{\Delta}{M} \tag{a6}$$

Δ and M are Christiansen's notation[2,23] (when simple cycles are involved). Δ is the product of forward rate constants minus the reverse ones. For example for a four step cycle ($i, j = 1-4$):

$$\Delta = k_1 k_2 k_3 k_4 - k_{-1} k_{-2} k_{-3} k_{-4} = e^{\sum_{i=1}^{N}(I_i - T_i)} \cdot [e^{-\Delta G} - 1] \tag{a7}$$

M can be expressed as the sum of all the terms in Christiansen's matrix ($\hat{M}$). This matrix can be formulated in the rate-constant representation as well as in the free-energy representation:

$$M = \sum_{a,b} M_{a,b} \tag{a8}$$

$$\begin{aligned} \hat{M} &= \begin{pmatrix} k_{-2}k_{-3}k_{-4} & k_2k_{-3}k_{-4} & k_2k_3k_{-4} & k_2k_3k_4 \\ k_1k_3k_4 & k_{-1}k_{-3}k_{-4} & k_{-1}k_3k_{-4} & k_{-1}k_3k_4 \\ k_1k_{-2}k_4 & k_1k_2k_4 & k_{-1}k_{-2}k_{-4} & k_{-1}k_{-2}k_4 \\ k_1k_{-2}k_{-3} & k_1k_2k_{-3} & k_1k_2k_3 & k_{-1}k_{-2}k_{-3} \end{pmatrix} \\ &= e^{\sum_{i=1}^{N}(I_i - T_i)} \begin{pmatrix} e^{T_1 - I_1} & e^{T_1 - I_2} & e^{T_1 - I_3} & e^{T_1 - I_4} \\ e^{T_2 - I_1 - \Delta G} & e^{T_2 - I_2} & e^{T_2 - I_3} & e^{T - I_4} \\ e^{T_3 - I_1 - \Delta G} & e^{T_3 - I_2 - \Delta G} & e^{T_3 - I_3} & e^{T_3 - I_4} \\ e^{T_4 - I_1 - \Delta G} & e^{T_4 - I_2 - \Delta G} & e^{T_4 - I_3 - \Delta G} & e^{T_4 - I_4} \end{pmatrix} \end{aligned}$$

This last matrix contains all the combinations of intermediates and transition states with an extra $-\Delta G$ term (the reaction free energy) in the cases that the intermediate comes before the transition state. The final expression of the TOF is then

$$\mathrm{TOF} = \frac{\Delta}{M} = \frac{e^{-\Delta G} - 1}{\sum_{i,j=1}^{N} e^{T_i - I_j - \delta G'_{i,j}}} \tag{a9}$$

$$\delta G'_{i,j} = \begin{cases} \Delta G & \text{if } i > j \\ 0 & \text{if } i \le j \end{cases}$$

A strict proof of this equation can be found in ref 11. As explained before, the numerator Δ expresses the driving force of the reaction, independent of the catalyst or the mechanism. When having an exothermic reaction with $\Delta G < 0$,

$$\Delta_{\text{exothermic}} = e^{-\Delta G} - 1 \approx e^{-\Delta G} \tag{a10}$$

resulting in (see Figure a1)

$$\mathrm{TOF}_{\mathrm{exothermic}}=\frac{\mathrm{e}^{-\Delta G}}{\sum_{i,j}\mathrm{e}^{T_i-I_j-\delta G'_{i,j}}}\approx \mathrm{e}^{-T_{\mathrm{TDTS}}+I_{\mathrm{TDI}}-\delta G}=\mathrm{e}^{-\delta E}$$

$$\delta G=\begin{cases}\Delta G & \text{if TDTS before TDI}\\ 0 & \text{if TDTS after TDI}\end{cases}\tag{a11}$$

In the case of an endothermic reaction with $\Delta G > 0$,

$$\Delta_{\mathrm{endothermic}}=\mathrm{e}^{-\Delta G}-1\approx -1\tag{a12}$$

with a TOF value of

$$\mathrm{TOF}_{\mathrm{endothermic}}=\frac{-1}{\sum_{i,j}\mathrm{e}^{T_i-I_j-\delta G'_{i,j}}}\approx -\mathrm{e}^{-T_{\mathrm{TDTS}}+I_{\mathrm{TDI}}-\delta G'}\tag{a13}$$

$$\delta G'=\begin{cases}\Delta G & \text{if TDTS after TDI}\\ 0 & \text{if TDTS before TDI}\end{cases}$$

So for endothermic reactions the TOF results are negative as expected, with an expression symmetrical to the one for an exothermic reaction (see Figure a1).

It is apparent that the free-energy representation leads to a simpler expression and a quicker identification of the two sates that determines the TOF of a catalytic cycle, whereas the rate-constant representation would be more cumbersome, involving products and quotients of a few rate constants.

Reactants and Products Concentrations. To add the reactants and products to the TOF analysis we can write the rate expressions as follows:

$$r=k_i[\mathrm{Cat}_{i-1}][\mathrm{R}_i]-k_{-i}[\mathrm{Cat}_i][\mathrm{P}_i]=k'_i[\mathrm{Cat}_{i-1}]-k'_{-i}[\mathrm{Cat}_i]\tag{a14}$$

where $i = 1, ..., N$.

The Δ terms becomes then

$$\begin{aligned}\Delta&=\prod k'_i-\prod k'_{-i}\\ &=\prod k_i[\mathrm{R}_i]-\prod k_{-i}[\mathrm{P}_i]\\ &=\prod \mathrm{e}^{I_{i-1}-T_i}[\mathrm{R}_i]-\prod \mathrm{e}^{I_i-T_i}[\mathrm{P}_i]\\ &=\mathrm{e}^{\sum_{i=1}^{N}(I_i-T_i)}\Big(\mathrm{e}^{-\Delta G}\prod_h[\mathrm{R}_h]-\prod_h[\mathrm{P}_h]\Big)\end{aligned}\tag{a15}$$

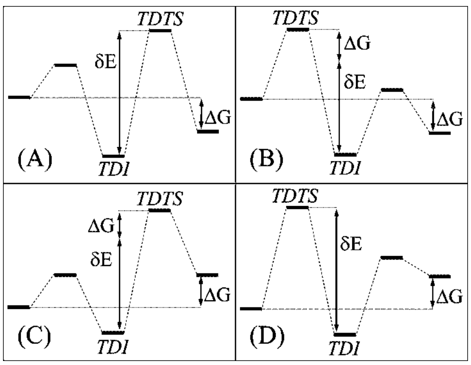

Figure a1. Graphic visualization of the energetic span for cases (A) and (B) in an exothermic reaction (eq a11) and (C) and (D) in an endothermic reaction (eq a13).

As before, the $M_{a,b}$ values can be expressed as exponentials of $(T_i - I_j)$:

$$M=\mathrm{e}^{\sum_{i=1}^{N}(I_i-T_i)}\cdot\Big(\sum_{i,j}\mathrm{e}^{T_i-I_j-\delta G'}\cdot\prod_h \delta R'_h\cdot\delta P_h\Big)\tag{a16}$$

$$\therefore \mathrm{TOF}=\frac{\mathrm{e}^{-\Delta G}\prod_h[\mathrm{R}_h]-\prod_h[\mathrm{P}_h]}{\sum_{i,j}\mathrm{e}^{T_i-I_j-\delta G'_{i,j}}\prod_h\delta R'_{h,i,j}\cdot\delta P_{h,i,j}}\tag{a17}$$

where each term in the summation corresponds to one of the $M_{a,b}$. In this expression, $\delta R'_{h,i,j}$ is $[\mathrm{R}_h]$ in the summation terms that came from the $M_{a,b}$ values, which include k'_h in it, and 1 elsewhere.

The ΔG value appears in $\delta G'_{i,j}$ when $i > j$, which corresponds to the $M_{a,b}$ values with k'_1. This is because we converted I_0 (that comes only from k'_1) to its equivalent $I_N - \Delta G$. ΔG and $[\mathrm{R}_1]$ appear if and only if k'_1 was included in the $M_{a,b}$ term (when $i > j$).

As the starting point is arbitrary in a cycle, a cyclic permutation $[p_h(i)]$ of the i and j indices gives the value of the other $\delta R'_{h,i,j}$:

$$\delta R'_{h,i,j}=\begin{cases}[\mathrm{R}_h] & \text{if } p_h(i)>p_h(j)\\ 1 & \text{if } p_h(i)\le p_h(j)\end{cases}\tag{a18}$$

being

$$p_h(i)=\begin{cases}i-h+1 & \text{if } i=h,h+1,...,N\\ i-h+1+N & \text{if } i=1,2,...,h-1\end{cases}\tag{a19}$$

Similarly, for the products $\delta P_{1,i,j} = [\mathrm{P}_1]$ in the summation terms that included in the $M_{a,b}$ the k'_{-1} rate constant. This comes when $i - 1 < j$. Again the cyclic permutation function is used:

$$\delta P_{h,i,j}=\begin{cases}[\mathrm{P}_h] & \text{if } p_h(i)<p_h(j)\\ 1 & \text{if } p_h(i)\ge p_h(j)\end{cases}\tag{a20}$$

Energetic Span Approximation with Reactants. The relation between the rate to the right and to the left of the global reaction is in the numerator of the TOF eq a17:

$$\begin{aligned}r&=\vec{r}-\overleftarrow{r}\\ \vec{r}&\propto \mathrm{e}^{-\Delta G}\prod[\mathrm{R}_h]\\ \overleftarrow{r}&\propto\prod[\mathrm{P}_h]\end{aligned}\tag{a21}$$

In equilibrium the rate in both directions is equal, so in consequence with well-known thermodynamic relations we have

$$\begin{aligned}\mathrm{e}^{-\Delta G}\prod[\mathrm{R}_h]_{\mathrm{eq}}-\prod[\mathrm{P}_h]_{\mathrm{eq}}&=0\\ \mathrm{e}^{-\Delta G}=\prod\frac{[\mathrm{P}_h]_{\mathrm{eq}}}{[\mathrm{R}_h]_{\mathrm{eq}}}&=K_{\mathrm{eq}}\end{aligned}\tag{a22}$$

For a successful reaction $\vec{r}$ is much greater than $\overleftarrow{r}$, and hence, the second term in the TOF numerator can be neglected for an exothermic reaction. In the same way, most often only one of the denominator's terms is significant, the one that connects the TDI and the TDTS (for instance a difference of 3 kcal/mol in the exponent makes one term 99% higher than other). As a result we get

$$\mathrm{TOF}\approx\frac{\mathrm{e}^{-\Delta G}\prod_h[\mathrm{R}_h]}{\mathrm{e}^{T_x-I_y-\delta G'_{x,y}}\prod_h\delta R'_{h,x,y}\delta P_{h,x,y}}\tag{a23}$$

$$\mathrm{TOF}\approx\mathrm{e}^{-\delta E}\prod_h\frac{\delta R_{h,x,y}}{\delta P_{h,x,y}}\tag{a24}$$

The reactants and products that appear in the reaction scheme are the ones that enter or leave the reaction between states I_y and T_x (going to the right), or mathematically:

$$\delta R_{h,i,j} = \begin{cases} [\mathrm{R}_h] & \text{if } p_h(i) \le p_h(j) \\ 1 & \text{if } p_h(i) > p_h(j) \end{cases}$$

$$\delta P_{h,i,j} = \begin{cases} [\mathrm{P}_h] & \text{if } p_h(i) < p_h(j) \\ 1 & \text{if } p_h(i) \ge p_h(j) \end{cases}$$

$$p_h(i) = \begin{cases} i-h+1 & \text{if } i = h, h+1, ..., N \\ i-h+1+N & \text{if } i = 1, 2, ..., h \end{cases} \tag{a25}$$

Appendix 2: Visual Technique for TDI and TDTS

A visual technique to define the TDI and TDTS is to graph two consecutive cycles (Figure a2). Look for each intermediate the maximum TS to the right of its position and measuring the energy gap between both states. The maximum gap will be the energetic span of the system.

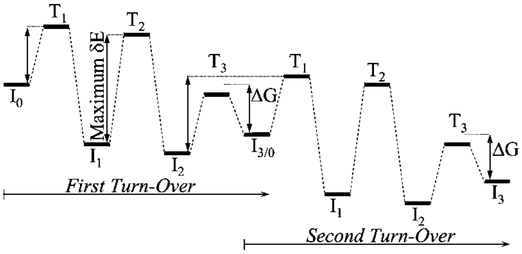

Figure a2. Graphical method to find the TDTS and TDI. From all possible combinations, I_1 and T_2 are the states that maximize the energetic span.

Appendix 3: Equivalence between Michaelis−Menten Model for Enzyme Catalysis and the Energetic Span Model

For the validation of the energetic span model we can verify its consistency with fully established kinetic models. Enzymes kinetics is discussed generally by use of the Michaelis−Menten representation (Figure a3, Scheme a1) that applies for a steady state situation where all the enzyme (E) bound intermediates have constant concentration with time.

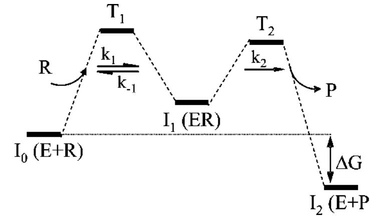

Figure a3. Energy profile for a Michaelis−Menten type enzymatic reaction.

SCHEME A1

$$\mathrm{E} + \mathrm{R} \underset{k_{-1}}{\overset{k_1}{\rightleftharpoons}} \mathrm{ER} \xrightarrow{k_2} \mathrm{E} + \mathrm{P}$$

The rate of the reaction is given by

$$r = \frac{r_{\mathrm{m}}[\mathrm{R}]}{K_{\mathrm{M}} + [\mathrm{R}]} \tag{a26}$$

Here r_{m} the maximum possible rate in the saturation kinetics (when changes in [R] do not affect r):

$$r_{\mathrm{m}} = k_2[\mathrm{E_t}] \qquad [\mathrm{E_t}] = [\mathrm{E}] + [\mathrm{ER}] \tag{a27}$$

Similarly, K_M is the so-called Michaelis−Menten constant,

$$K_{\mathrm{M}} = \frac{k_{-1} + k_2}{k_1} \tag{a28}$$

characteristic of the enzyme.

Let us try now to derive the TOF equivalent of the Michaelis−Menten equation. By converting the rate constants to energies, we can express the Michaelis−Menten TOF as

$$\begin{aligned} \mathrm{TOF_{MM}} = \frac{r}{[\mathrm{E_t}]} &= \frac{\mathrm{e}^{I_1-T_2}[\mathrm{R}]}{\dfrac{\mathrm{e}^{I_1-T_1} + \mathrm{e}^{I_1-T_2}}{\mathrm{e}^{I_2-T_1-\Delta G}} + [\mathrm{R}]} \\ &= \frac{\mathrm{e}^{-\Delta G}[\mathrm{R}]}{\mathrm{e}^{T_2-I_2} + \mathrm{e}^{T_1-I_2} + \mathrm{e}^{T_2-I_1-\Delta G}[\mathrm{R}]} \end{aligned} \tag{a29}$$

In our kinetic model the full two steps reaction is (see eq 7)

$$\mathrm{TOF} = \frac{\mathrm{e}^{-\Delta G}[\mathrm{R}] - [\mathrm{P}]}{\mathrm{e}^{T_2-I_2} + \mathrm{e}^{T_1-I_2} + \mathrm{e}^{T_2-I_1-\Delta G}[\mathrm{R}] + \mathrm{e}^{T_1-I_1}[\mathrm{P}]} \tag{a30}$$

From here the equivalence of the energetic span model equation (eq a30) to the Michaelis−Menten model (eq a29) is clear, with the exception that the terms with the product concentration are neglected in the Michaelis−Menten model.

Acknowledgment. This research is supported by the DFG within the framework of the German Israeli Project Cooperation (DIP). This paper is dedicated to Avinoam Ben-Shaul on the occasion of his 65th birthday. His contributions in the field of biophysics are greatly appreciated.

Supporting Information Available: Excel file that calculates TOF. This material is available free of charge via the Internet at http://pubs.acs.org.

References and Notes

(1) See, for example: (a) Maseras, F., Lledos, A., Eds. *Computational Modeling of Homogeneous Catalysis*; Kluwer Academic Publishers: Amsterdam, 2002. (b) Truhlar, D. G., Morokuma, K., Eds. *Transition State Modeling for Catalysis*; American Chemical Society: Washington, DC, 1998. (c) Shaik, S.; Kumar, D.; de Visser, S. P.; Altun, A.; Thiel, W. *Chem. Rev.* **2005**, *105*, 2279. (d) Frenking, G.; Fröhlich, N. *Chem. Rev.* **2000**, *100*, 717. (e) Cundari, T. R.; Deng, J.; Fu, W.; Klinckman, T. R.; Yoshikawa, A. *J. Chem. Inf. Comput. Sci.* **1998**, *38*, 941. (f) Neurock, M. *J. Catal.* **2003**, *216*, 73. (g) Gokhale, A. A.; Kandoi, S.; Greeley, J. P.; Mavrikakis, M.; Dumesic, J. A. *Chem. Eng. Sci.* **2004**, *59*, 4679. (h) Boudart, M. *Catal. Lett.* **2000**, *65*, 1. (i) Greeley, J.; Mavrikakis, M. *Nat. Mater.* **2004**, *3*, 810. (j) Sundermann, A.; Uzan, O.; Martin, J. M. L. *Chem. Eur. J.* **2001**, *7*, 17030. (k) Braga, A.; Morgon, N.; Ujaque, G.; Maseras, F. *J. Am. Chem. Soc.* **2005**, *127*, 9298. (l) Senn, H. M.; Ziegler, T. *Organometallics* **2004**, *23*, 2980. (m) Hellman, A.; Baerends, E. J.; Biczysko, M.; Bligaard, T.; Christensen, C. H.; Clary, D. C.; Dahl, S.; van Harrevelt, R.; Honkala, K.; Jonsson, H.; Kroes, G. J.; Luppi, M.; Manthe, U.; Norskov, J. K.; Olsen, R. A.; Rossmeisl, J.; Skulason, E.; Tautermann, C. S.; Varandas, A. J. C.; Vincent, J. K. *J. Phys. Chem. B* **2006**, *110*, 17719. (n) Goossen, L. J.; Koley, D.; Hermann, H. L.; Thiel, W. *Organometallics* **2006**, *25*, 54. (o) Goossen, L. J.; Koley, D.; Hermann, H. L.; Thiel, W. *J. Am. Chem. Soc.* **2005**, *127*, 11102. (p) Noodleman, L.; Lovell, T.; Han, W.; Li, J.; Himo, F. *Chem. Rev.* **2004**, *104*, 459. (q) Niu, S.; Hall, M. B. *Chem. Rev* **2000**, *100*, 353. (r) Honkala, K.; Hellman, A.; Remediakis, I. N.; Logadottir, A.; Carlsson, A.; Dahl, S.; Christensen, C. H.; Nørskov, J. K. *Science* **2005**, *307*, 555.

(2) Christiansen, J. A. *Adv. Catal.* **1953**, *5*, 311.

(3) (a) Boudart, M. *J. Phys. Chem.* **1983**, *87*, 2786. (b) Holstein, W. L.; Boudart, M. *J. Phys. Chem.* **1997**, *101*, 9991. (c) Dumesic, J. A. *J. Catal.* **1999**, *185*, 496.

(4) Cortright, R. D.; Dumesic, J. A. *Adv. Catal.* **2001**, *46*, 161.

(5) (a) Campbell, C. T. *Topics Catal.* **1994**, *1*, 353. (b) Campbell, C. T. *J. Catal.* **2001**, *204*, 520.

(6) Baranski, A. *Solid State Ionics* **1999**, *117*, 123.

(7) Campbell, C. T. *J. Catal.* **2001**, *204*, 520.

(8) Dumesic, J. A. *J. Catal.* **2001**, *204*, 525.

(9) Bligaard, T.; Nørskov, J. K.; Dahl, S.; Matthiesen, J.; Christensen, C. H.; Sehested, J. *J. Catal.* **2004**, *224*, 206.

(10) Boisen, A.; Dahl, S.; Nørskov, J. K.; Christensen, C. H. *J. Catal.* **2005**, *230*, 309.

(11) Kozuch, S.; Shaik, S. *J. Am. Chem. Soc.* **2006**, *128*, 3355.

(12) (a) The TDI was the previously called MARI (Most Abundant Reaction Intermediate). See ref 11 and : Stolze, P. *Prog. Surf. Sci.* **2000**, *65*, 65. (b) Boudart, M.; Djéga-Mariadassou, G. *J. Catal.* **2003**, *216*, 89.

(13) The TDTS was previously called RDTS (Rate Determining Transition State). See ref 11.

(14) Amatore, C.; Jutand, A. *J. Organomet. Chem.* **1999**, *576*, 254.

(15) Kozuch, S.; Jutand, A.; Amatore, C.; Shaik, S. *Organometallics* **2005**, *24*, 2319.

(16) (a) Molina, M. J.; Rowland, F. S. *Nature* **1974**, *249*, 810. (b) Cicerone, R. J.; Stolarski, R. S.; Walters, S. *Science* **1974**, *185*, 1165.

(17) All calculations are free energies at 220 K and 0.1 atm, at the pw91/aug-cc-pVQZ level, based on the cis catalytic cycle of : Tyrrell, J.; Kar, T.; Bartolotti, L. J. *J. Phys. Chem. A* **2001**, *105*, 4065.

(18) Cohen, S.; Kozuch, S.; Hazan, C.; Shaik, S. *J. Am. Chem. Soc.* **2006**, *128*, 11028.

(19) (a) Ortiz de Montellano, P. R., Ed. *Cytochrome P450: Structure, Mechanism and Biochemistry*, 2nd ed.; Plenum Press: New York, 1995. (b) Ortiz de Montellano, P. R., Ed. *Cytochrome P450: Structure, Mechanism and Biochemistry*, 3rd ed.; Kluwer Academic/Plenum Publishers: New York, 2005.

(20) Mayer, J. M. *Acc. Chem. Res.* **1998**, *31*, 441.

(21) Jacobsen, C. J. H.; Dahl, S.; Clausen, B. S.; Bahn, S.; Logadottir, A.; Nørskov, J. K. *J. Am. Chem. Soc.* **2001**, *123*, 8404.

(22) Nørskov, J. K.; Bligaard, T.; Logadottir, A.; Bahn, S.; Bollinger, M.; Hansen, L. B.; Bengaard, H.; Hammer, B.; Sljivancanim, Z.; Mavrikakis, M.; Xu, Y.; Dahl, S.; Jacobsen, J. H. *J. Catal.* **2002**, *209*, 275.

(23) Boudart, M. *Kinetics of Chemical Processes*; Prentice Hall Inc.: Englewood Cliffs, NJ, 1968; p 67.

(24) *A TOF Calculation device:* An excel file that calculates the TOF from the energy of the states is available as Supporting Information, or from the authors upon request.

JP8004772